JOURNAL OF THERMOPHYSICS AND HEAT TRANSFER
Vol. 16, No. 4, October–December 2002

Influence of the Alternating Power Supply Component on Plasma Arc Characteristic

Wenhua Zhao,* Liming Chen,† and Guanzhong Zhang‡
Tsinghua University, 100084 Beijing, People's Republic of China

The influences of the alternating component of the power supply on the arc blow force and the heat transfer to the anode are studied experimentally and theoretically. The alternating component has a great influence on the time-averaged total pressure of the plasma flow in the dc arc, thus influencing the arc blow force. The open-circuit voltage of the three-phase all-wave silicon rectifier power supply has an influence on the magnitude of the alternating component and, therefore, influences the heat transfer to the transferred anode. At present, the three-phase all-wave silicon rectifier power supply is the necessary facility in the study of large power plasma arcs, which have been widely used in aeronautics, astronautics, and industrial fields, and so the conclusions obtained are helpful for scientific research and industrial practice.

Nomenclature

$\boldsymbol{B}$	=	magnetic induction, T
Cp	=	specific heat of water, J/(kg · °C)
E	=	axial component of the electric field intensity of the arc, V/m
G	=	flow rate of water, kg/s
I	=	current of the arc, A
$\boldsymbol{j}$	=	current density, A/m^2
k	=	Boltzmann constant, 1.380658×10^{-23} J/k
m_i	=	mass of the primary ion, kg
n	=	total particle number density, m^{-3}
n_i	=	number density of the primary ion, m^{-3}
P	=	pressure, Pa
P_{atm}	=	pressure of the atmosphere, Pa
P_{total}	=	total pressure, Pa
$P_{0(z)}$	=	static pressure at the axes of the arc, varying with axial position z, Pa
P_Σ	=	excess total pressure, Pa
$P_{\Sigma\text{theo}(z)}$	=	theoretical excess total pressure, Pa
$P_{\infty(z)}$	=	static pressure at boundary of the arc electrical conduction $R^*_{(z)}$, varying with the axial position z, Pa
Q	=	total heat flow transferred to anode, J/s
$R^*_{(z)}$	=	boundary of the arc electrical conduction, varying with the axial position z, m
r	=	radius of the arc, m
T_0	=	temperature at the axes of the plasma arc, K
$T_{0(z)}$	=	temperature at the axes of the arc, varying with the axial position z, K
t	=	water temperature, °C
u	=	axial component of the plasma velocity, m/s
u_0	=	axial component of plasma velocity at the axes of the arc, m/s
u_∞	=	axial component of plasma velocity at the arc boundary, m/s
v	=	radial component of plasma velocity, m/s
η	=	heating efficiency
μ	=	viscosity coefficient, kg/(m · s)
μ_e	=	magnetic permeability of the plasma, H/m
ρ	=	plasma density, kg/m^3
ρ_0	=	density at the axes of the arc, kg/m^3
τ_E^{--}	=	relaxation time of electron, s
τ_E^{++}	=	relaxation time of ion, s
τ_E^{-+}	=	relaxation time of electron ion, s
ω	=	pulse angular frequency, rad/s

Subscripts

in	=	inlet of cooling water of the anode
out	=	outlet of cooling water of the anode
r	=	radial component of cylindric coordinate
water	=	water
z	=	axial component of cylindric coordinate
148V	=	open circuit voltage of the experiments
315V	=	open circuit voltage of the experiments
φ	=	circumferential component of cylindric coordinate

Received 10 December 2001; revision received 30 May 2002; accepted for publication 30 May 2002.

*Professor, Department of Engineering Mechanics; zhaowh@mail.tsinghua.edu.cn.
†Graduate Student, Department of Engineering Mechanics.
‡Associate Professor, Department of Engineering Mechanics.

I. Introduction

ARC plasma has been widely used in aeronautics and astronautics. A great deal of work on the pulsation of plasma, the characteristics of the dc arc, and the characteristics of the ac arc has been done in recent years.[1–7] For example, the flow status of an arc in a channel has been studied in detail. The study in Ref. 3 indicated that the arc in a channel was steady and that the flow in the arc is laminar for a certain distance from the cathode. Then after a transition area, the arc became unsteady, and the flow became turbulent. These phenomena were observed and photographed. However, work on the influence of the alternating component of the dc arc power supply on the arc characteristic is infrequent, and the influence of open-circuit voltage on the alternating component of current and voltage is seldom described. In Ref. 8, Zhao et al. have studied the effect of power supply characteristics on the arc plasma jet. In this paper, the experimental and theoretical investigations focus on the influence of the alternating component of the arc voltage of the dc arc on the arc characteristic. The experiments show that the alternating component not only influences the arc inner flow, but also influences the heat transfer to anode and other parameters of the arc characteristic. Thus, the alternating component of the dc arc voltage should be considered as one of the parameters that influence the arc characteristic.

II. Experimental Setup

The experimental setup is shown in Fig. 1. The gas is supplied along the axes of the plasma generator (1; Fig. 1). The cathode

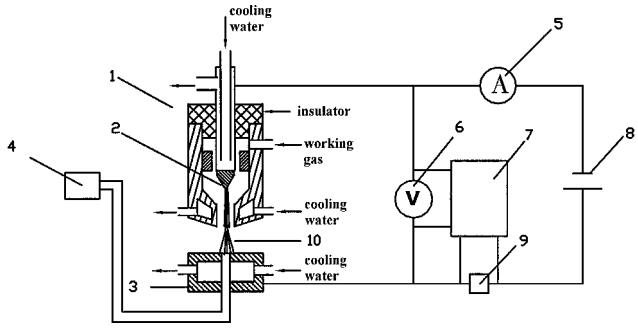

Fig. 1 Schematic diagram of experimental setup: 1, plasma generator; 2, cerium–tungsten cathode; 3, transferred anode; 4, pressure transducer; 5, amperemeter; 6, voltmeter; 7, oscillograph; 8, dc power supply; 9, water-cooled resistance; and 10, plasma arc.

(2; Fig. 1) and nozzle are cooled with water. As a probe for measuring the total pressure of the arc, a hole with a 1-mm diam is in the center of the water-cooled transferred anode (3; Fig. 1), and the transducer (4; Fig. 1) translates the pressure signals to electric signals. In the experiments, the transducer measures the time-averaged pressure value. The power supply is a three-phase all-wave silicon rectifier welding set (8; Fig. 1). The time-averaged, open-circuit voltages are 315 ± 5 and 148 ± 5 V. When the open-circuit voltage of the power supply is changed, different alternating components of the arc voltage can be obtained. The working voltages and currents of the arc are measured by a dc voltmeter and a dc amperemeter (6 and 5, respectively; Fig. 1). A water-cooled resistance (9; Fig. 1) of 0.2 Ω is in series with the circuit to measure accurately the current and the alternating component. The voltage signals of the resistance are input into an oscillograph; then, the currents and their alternating components are recorded.

The flow rate of the water that cools the transferred anode and the water temperatures at the inlet and the outlet are measured to get the heat flow transferred to the anode.

Argon is used as the working gas in the experiments, and the flow rate is 0.196 g/s. The diameter of the nozzle of the plasma generator is 6 mm. The distance between the tip of the cathode and the outlet of the nozzle is 7 mm, and the distance between the outlet of the nozzle and the transferred anode is 8 mm.

III. Experimental Results

The experiments indicate that the difference of the open-circuit voltages does not affect the steady current–voltage characteristics of the arc at the same flow rate of argon, as shown in Fig. 2. This conclusion is consistent with that of other references.[9,10] However, the same steady current–voltage characteristics does not mean the same arc characteristic. The experiments of this paper indicate that there are different total arc pressures and different heat flows transferred to the anode.

A. Pulse Waveforms of Voltage and Current of Plasma Arc

The variation of the voltage and the current of the arc with the time is recorded with the oscillograph. The recorded waveforms of the voltage and the current at the average current of 100 A are showed in Fig. 3. It is shown in Fig. 3 that the voltage and current of the arc fluctuate with time. Generally, the fluctuation is related to the fluctuation in the dc power supply and the flow status of plasma arc. In our experiments, the arc is relatively short (15 mm). It is observed that the arc is steady. According to the estimation of the Reynolds number, the flow in the arc is laminar and has little effect on the fluctuations of the voltage and current of the arc. Then the fluctuations are attributed to the fluctuation in the dc power supply. In Fig. 3, the pulse waveforms of the voltage and the current can be approximately described as sine waveforms. The frequency is 300 Hz. It is just the frequency of the alternating component of the three-phase all-wave silicon rectifier welding set. The reason for the large amplitude of the pulsation is mainly related to the arc characteristic.

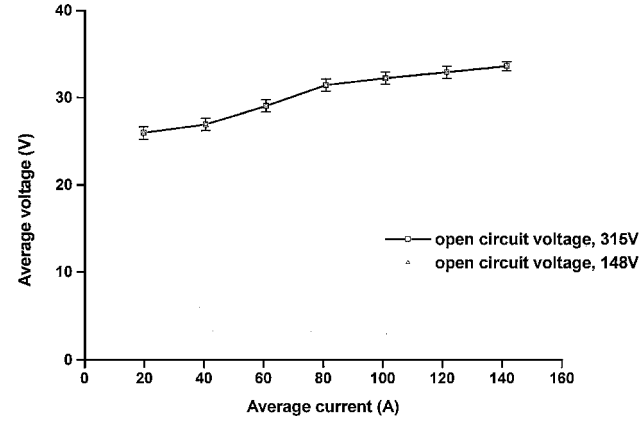

Fig. 2 Steady current–voltage characteristics of argon arc at different open-circuit voltages and the same argon flow rate.

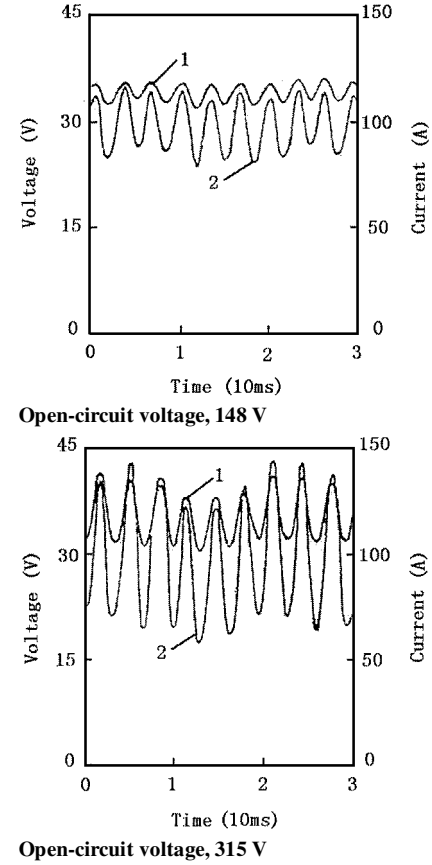

Fig. 3 Voltage and current waveforms of arc plasma: 1, voltage waveform and 2, current waveform.

The conclusions obtained from Fig. 3 follow:

1) The higher open-circuit voltage leads to the larger alternating component of the voltage and the current of the arc.

2) The phase difference between the waveform of the voltage and that of the current is very small. That means the heat inertia is rather small.

3) A large alternating component of the voltage leads to a large amplitude of current pulsation. For example, when the average arc current is 100 A and the open-circuit voltage is 315 V, the amplitude of current pulsation can be as large as 72 A.

B. Excess Total Pressure on Transferred Anode

The time-averaged excess total pressure on a transferred anode can be expressed as

$$P_{\Sigma} = P_{\text{total}} - P_{\text{atm}} \tag{1}$$

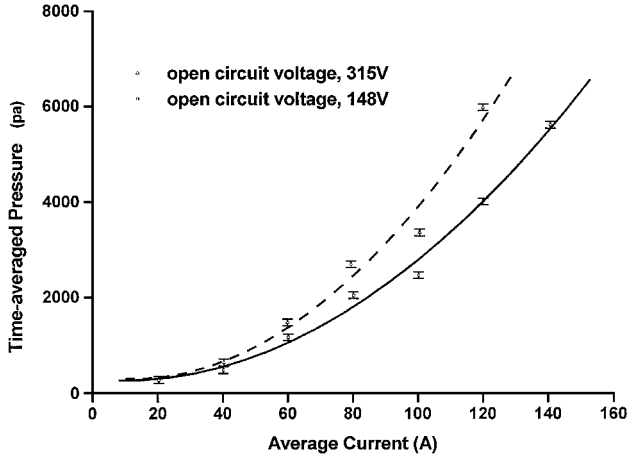

Fig. 4 Time-averaged excess total pressure at the stagnation point on the transferred anode at different open-circuit voltages.

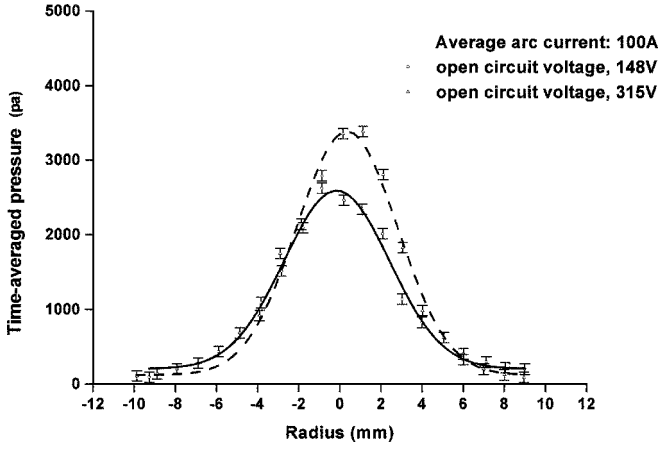

Fig. 5 Radial distribution of the axial component of the time-averaged excess total pressure on the transferred anode at different open-circuit voltages.

To measure the total pressure at the stagnation point on the transferred anode, the hole for the pressure measurement on the transferred anode is aligned with the axes of the arc. Different alternating components can be obtained by changing the open-circuit voltages. The variation of the time-averaged excess total pressure with the average currents is shown in Fig. 4. In this procedure, the gas flow rate and other conditions were kept unchanged as mentioned earlier. Figure 4 indicates that the time-averaged arc excess total pressure at the stagnation point on the transferred anode increases with the rising of the alternating component of the arc voltage corresponding to larger open-circuit voltage, as does the arc blow force. Figure 4 shows that some experimental points deviate from the fitting curve. The reason is that the size and the position of the cathode spot on the cathode surface are changing with the ablation of the cathode, especially in large current.

The distribution of the time-averaged excess total pressure on the transferred anode is measured by moving the plasma generator breadthwise. When the hole is aligned with the axes of the arc, it measures the excess total pressure at the stagnation point. When the hole is not aligned with the axes of the arc, it measures the axial component of the excess total pressure. Nevertheless, it can represent the distribution of the arc blow force on the anode by the arc. Figure 5 indicates that there are similar curve shapes of the distribution for large and small current alternating components corresponding to high and low open-circuit voltages, but the arc blow force is larger for larger current alternating component.

C. Heat Transfer to Anode

From the flow rate of the water cooling the transferred anode and the water temperatures at the inlet and the outlet, the total heat flow

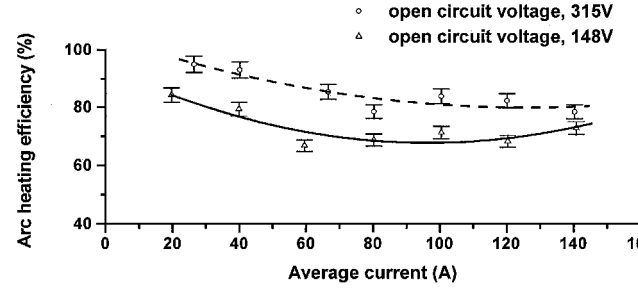

Fig. 6 Arc heating efficiency to the anode at different open-circuit voltages.

transferred to the anode from plasma arc can be calculated. When the total heat flows at different alternating components of the arc voltage corresponding to different open-circuit voltages and at the same average currents are compared, it is found that the total heat flow is larger at high open-circuit voltage than that at low open-circuit voltage when the average currents are the same, namely,

$$\frac{Q_{315\mathrm{V}}}{Q_{148\mathrm{V}}} = \frac{[C_p \cdot G_{\mathrm{water}}(t_{\mathrm{out}} - t_{\mathrm{in}})]_{315\mathrm{V}}}{[C_p \cdot G_{\mathrm{water}}(t_{\mathrm{out}} - t_{\mathrm{in}})]_{148\mathrm{V}}} > 1 \tag{2}$$

Because the arc current–voltage characteristics are the same at different alternating components, they have the same power. If the numerator and denominator in expression (2) are divided by the arc power, then the ratio of the heating efficiencies at different alternating components corresponding to different open-circuit voltages is obtained, namely,

$$\eta_{315\mathrm{V}}/\eta_{148\mathrm{V}} > 1 \tag{3}$$

Figure 6 shows the comparative curves of heating efficiency at two different alternating components corresponding to two different open-circuit voltages. From the curves some conclusions can be reached:

1) Generally, the heating efficiency of the transferred arc to the anode is higher than that of plasma jet.

2) The heating efficiency decreases with the rising of the average current.

3) In the current range of the experiments, the heating efficiency to the anode increases with the rising of the alternating component of the arc voltage and the arc current. This is because of the higher velocity of the plasma in the arc corresponding to the higher excess total pressure and blow force as mentioned earlier.

D. Arc Diameter at Different Alternating Components

The time-averaged illuminant diameter of the arc is measured by photography. The measurement shows that the alternating component hardly affects the time-averaged diameter when the average arc currents are the same at the currents of 20, 40, 60, 100, 120, 140, and 160 A. Figure 7 shows the average illuminant diameters of the arc at 4 mm away from the nozzle. The conclusions are as follows:

1) The alternating component does not affect the average illuminant diameter of the arc.

2) If the average current is lower than 120 A, the time-averaged illuminant diameters of the arc increases with the rising of the currents; if the average current is higher than 120 A, the time-averaged illuminant diameters of the arc are almost invariable in the current range of our experiments.

IV. Theorectical Calculation and Analysis of the Arc Characteristic

To explain qualitatively the experimental results, theoretical calculation and analysis are performed. Before the theoretical analysis, two assumptions are made. The first is that the experiments are conducted in a state of thermal equilibrium; the second is that the flow in the arc is laminar. To justify the first assumption, the relaxation time of the plasma in the experiments is calculated. First, the temperature at the axes of the plasma arc is estimated. If the displacement

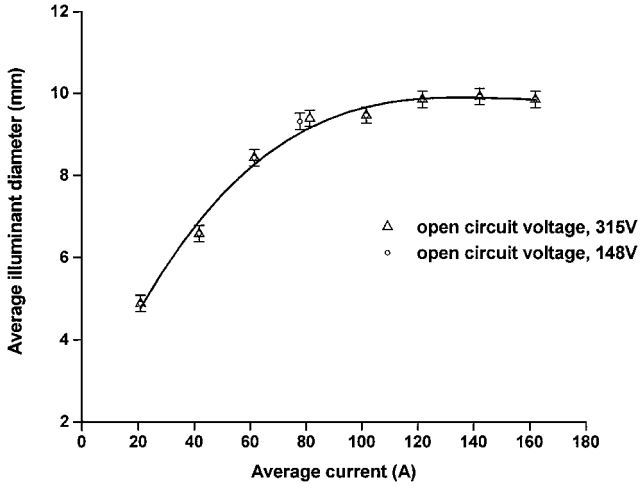

Fig. 7 Variation of the time-averaged illuminant diameter of the arc with the current at two different open-circuit voltages.

current is neglected, if the electronic current is regarded as the main factor for conducting current, and if the plasma mainly consists of electrons and primary ions, then the temperature at the axes of the plasma arc can be estimated with existing methods[11–13]:

$$T_0 = 1.04 \times 10^3 [I/R^2 E]^{\frac{2}{3}} \tag{4}$$

If the diameter of the nozzle is considered on average as the diameter of the arc, the calculation shows that the temperature at the center of the arc is about 20,000 K. Under atmospheric conditions atmosphere and the temperature of argon, 20,000 K, the relaxation times of τ_E^{--}, τ_E^{++}, and τ_E^{-+} are estimated according to formulas (10-101), (10-102), and (10-103) in Ref. 14, that is, $\tau_E^{-+} \sim 10^{-9}$, $\tau_E^{--} \sim 10^{-14}$, and $\tau_E^{++} \sim 10^{-12}$ s. The pulse frequency of the voltage and the current is 300 Hz. Thus, the variational time of macroparameters due to the pulsation of the voltage and the current has the order of magnitude of 10^{-3} s. It is much larger than the relaxation time of the plasma. Also, in the core of the arc the qualitative length in which plasma parameters have apparent changes is obviously greater than the mean free path of the particles. Therefore, under the condition of pulsations of the voltage and the current, the thermal equilibrium of the arc exists in the core of the arc.

The experiments show that the voltage and the current of the arc have approximately the same pulse frequencies and phases. This indicates that the macroparameters of the arc pulsate in the same frequency as that of the voltage and the current at least in the core of the arc where the electrical conductivity and the temperature are high enough. However, the time-averaged illuminant diameters of the arc are same at two different alternating components corresponding to two different open-circuit voltages. Thus, the effect of the pulsations of the voltage and the current at the boundary of the arc is small. This indicates that the thermal inertia is relatively small in the core of the arc and relatively large at the boundary.

The second assumption that the flow in the arc is laminar is also reasonable. In Ref. 3, it was indicated that the arc was steady and that the flow in the arc was laminar in a certain length range. In our experiments, the length of the arc is relatively short (15 mm). Note that the arc is steady, and the Reynolds number is $360 \sim 890$, so that the assumption of laminar flow in the arc is justified.

In accordance with the preceding analysis, the effect of the alternating component on the arc blow force is estimated in the following paragraphs.

Argon gas is fed into the plasma generator paralleling the axes of the transferred arc. The equations of the axisymmetric arc are represented in the form of cylindric coordinates r, φ, and z:

$$\rho v \frac{\partial u}{\partial r} + \rho u \frac{\partial u}{\partial z} = -\frac{\partial P}{\partial z} + (\boldsymbol{j} \times \boldsymbol{B})_z + \frac{1}{r}\frac{\partial}{\partial r}\left(r\mu \frac{\partial u}{\partial r}\right) \tag{5}$$

$$\frac{\partial P}{\partial r} = (\boldsymbol{j} \times \boldsymbol{B})_r \tag{6}$$

Because $\partial/\partial\phi = 0$, Ampere's law is

$$\mu_e j_r = -\frac{\partial B_\varphi}{\partial z}, \qquad \mu_e j_z = \frac{1}{r}\frac{\partial}{\partial r}(r B_\varphi) \tag{7}$$

It is supposed that the circumferential current density is zero, that is, $j_\phi = 0$. Thus,

$$(\boldsymbol{j} \times \boldsymbol{B})_z = j_r B_\varphi, \qquad (\boldsymbol{j} \times \boldsymbol{B})_r = -j_z B_\varphi \tag{8}$$

Using the boundary condition

$$B_\phi = 0, \qquad r = 0 \tag{9}$$

and integrating the second formula of Eq. (7), one obtains

$$B_\varphi = \frac{\mu_e}{r}\int_0^r j_z r \, \mathrm{d}r \tag{10}$$

Substitution of Eq. (10) into Eq. (6) results in

$$\frac{\partial P}{\partial r} = -\frac{\mu_e j_z}{r}\int_0^r j_z r \, \mathrm{d}r \tag{11}$$

Integrating Eq. (11) leads to

$$P_{(r,z)} = P_{0(z)} - \frac{\mu_e}{2\pi}\int_0^r \frac{j_z}{r}\left(\int_0^r 2\pi j_z r \, \mathrm{d}r\right)\mathrm{d}r \tag{12}$$

At the boundary of the arc electrical conduction $R^*_{(z)}$,

$$P = P_{\infty(z)} \tag{13}$$

one obtains

$$P_{0(z)} = P_{\infty(z)} + \frac{\mu_e}{2\pi}\int_0^{R^*_{(z)}} \frac{j_z}{r}\left(\int_0^r 2\pi j_z r \, \mathrm{d}r\right)\mathrm{d}r \tag{14}$$

Substituting the expressions in Eq. (14) into Eq. (12), we obtain the following expression:

$$P_{(r,z)} = P_{\infty(z)} + \frac{\mu_0}{2\pi}\int_r^{R^*_{(z)}} \frac{j_z}{r}\left(\int_0^r 2\pi j_z r \, \mathrm{d}r\right)\mathrm{d}r \tag{15}$$

Thus, the excess static pressure at the axes of the arc can be expressed as

$$P_{0(z)} - P_{\infty(z)} = \frac{\mu_e}{2\pi}\int_0^{R^*_{(z)}} \frac{j_z}{r}\left(\int_0^r 2\pi j_z r \, \mathrm{d}r\right)\mathrm{d}r \tag{16}$$

If the distribution of the current density is known, the distribution of the static pressure of the arc can be immediately obtained. Therefore, it is assumed that the distribution of the current density is

$$j_z = I A_{1(z)} A_{2(r)} \tag{17}$$

where $A_{1(z)}$ is a function of z and $A_{2(r)}$ is a function of r.

This satisfies

$$\int_0^{R^*_{(z)}} 2\pi I A_{1(r)} A_{2(r)} r \, \mathrm{d}r = I \tag{18}$$

then we have

$$P_{0(z)} - P_{\infty(z)} = \frac{\mu_e I^2}{2\pi}\int_0^{R^*_{(z)}} \frac{1}{r} A_{1(z)} A_{2(r)}\left(\int_0^r 2\pi A_{1(z)} A_{2(r)} r \, \mathrm{d}r\right)\mathrm{d}r \tag{19}$$

which indicates that the excess static pressure at the axes of the arc is proportional to the square of the current. $R^*_{(z)}$ can be expressed as $Z_{(R^*)}$ in the form of an inverse function. On the assumption that

$$\aleph_{(R^*)} = \int_0^{R^*_{(z)}} \frac{1}{r} A_{1(z)} A_{2(r)} \left(\int_0^r 2\pi A_{1(z)} A_{2(r)} r \, \mathrm{d}r \right) \mathrm{d}r \tag{20}$$

Eq. (19) can be expressed as follows:

$$P_{0(z)} - P_{\infty(z)} = \left(\mu_e I^2 / 2\pi\right) \aleph_{(R^*)} \tag{21}$$

To obtain the flow velocity u of the plasma in the arc, Eq. (5) can be expressed as follows by combining Eqs. (5), (8), and (15):

$$\rho v \frac{\partial u}{\partial r} + \rho u \frac{\partial u}{\partial z} = -\frac{\partial p_{\infty(z)}}{\partial z} - \frac{\partial}{\partial z} \left[\frac{\mu_e}{2\pi} \int_r^{R^*_{(Z)}} \frac{j_z}{r} \left(\int_0^r 2\pi j_z r \, \mathrm{d}r \right) \mathrm{d}r \right]$$

$$+ j_r B_\varphi + \frac{1}{r} \frac{\partial}{\partial r} \left(r\mu \frac{\partial u}{\partial r} \right) \tag{22}$$

By combining the first formula of Eq. (7) and Eq. (10), we have

$$j_r B_\varphi = -\frac{\mu_e}{2} \frac{\partial}{\partial z} \left(\frac{1}{r} \int_0^r j_z r \, \mathrm{d}r \right)^2 \tag{23}$$

thus, Eq. (22) can be expressed as follows:

$$\rho v \frac{\partial u}{\partial r} + \rho u \frac{\partial u}{\partial z} = -\frac{\partial p_{\infty(z)}}{\partial z} - \frac{\partial}{\partial z} \left[\frac{\mu_e}{2\pi} \int_0^{R^*_{(z)}} \frac{j_z}{r} \left(\int_0^r 2\pi j_z r \, \mathrm{d}r \right) \mathrm{d}r \right]$$

$$- \frac{\mu_e}{2} \frac{\partial}{\partial z} \left(\frac{1}{r} \int_0^r j_z r \, \mathrm{d}r \right)^2 + \frac{1}{r} \frac{\partial}{\partial r} \left(r\mu \frac{\partial u}{\partial r} \right) \tag{24}$$

In the experiments where the gas flow rate and the velocity are low, the inertia force item can be neglected. Electromagnetic force can be regarded as in balance with the viscous force, and then Eq. (24) can be simplified as follows:

$$\frac{1}{r} \frac{\partial}{\partial r} \left(r\mu \frac{\partial u}{\partial r} \right) = \frac{\partial}{\partial z} \left[\frac{\mu_e}{2\pi} \int_r^{R^*_{(z)}} \frac{j_z}{r} \left(\int_0^r 2\pi j_z r \, \mathrm{d}r \right) \mathrm{d}r \right]$$

$$+ \frac{\mu_e}{2} \frac{\partial}{\partial z} \left(\frac{1}{r} \int_0^r j_z r \, \mathrm{d}r \right)^2 \tag{25}$$

Thus,

$$u - u_\infty = \int_{R^*_{(z)}}^r \frac{\mu_e}{4\pi^2 r \mu}$$

$$\times \frac{\partial}{\partial z} \left\{ \int_0^r \left[\int_r^{R^*_{(z)}} \frac{1}{r^3} \left(\int_0^r 2\pi j_z r \, \mathrm{d}r \right)^2 \mathrm{d}r \right] r \, \mathrm{d}r \right\} \mathrm{d}r \tag{26}$$

Substituting the expression in Eq. (17) into Eq. (26), we can obtain the excess velocity at the axes of the arc

$$u_0 - u_\infty = \frac{\mu_e I^2}{4\pi^2} \int_{R^*_{(z)}}^0 \frac{1}{\mu r}$$

$$\times \frac{\partial}{\partial z} \left\{ \int_0^r \left[\int_r^{R^*_{(z)}} \frac{1}{r^3} \left(\int_0^r 2\pi A_{1(z)} A_{2(r)} r \, \mathrm{d}r \right)^2 \mathrm{d}r \right] r \, \mathrm{d}r \right\} \mathrm{d}r \tag{27}$$

According to Ref. 15, we select the following expression of viscosity with the temperature from 5000 to 11,000 K:

$$\mu = \mu_0 (T / T_0) \tag{28}$$

where $\mu_0 = 1.8 \times 10^{-3}$ g/cm · s and $T_0 = 5000$ K. For the sake of convenience, Eq. (28) can be expressed as

$$\mu = MT \tag{29}$$

where $M = \mu_0 / T_0$.

The distribution of the arc temperature can be represented with the expression related to the temperature at the axes of the arc,

$$T = T_{0(z)} A_{3(z)} A_{4(r)} \tag{30}$$

where $A_{3(z)}$ is a function of z and $A_{4(r)}$ is a function of r.

Because j is related to T, all of $T_{0(z)}$, $A_{3(z)}$, and $A_{4(r)}$ should be selected according to the relation between $A_{1(z)}$ and $A_{2(r)}$. Substitution of Eqs. (29) and (30) into Eq. (27) results in

$$u_0 - u_\infty = \frac{\mu_e I^2}{4\pi^2 T_0 M} K \left(A_{1(z)}, A_{3(z)}, R^*_{(z)} \right) \tag{31}$$

where the K can be obtained by the integration of the following formula:

$$K \left(A_{1(z)}, A_{3(z)}, R^*_{(z)} \right) = \int_{R^*}^0 \frac{1}{r A_{3(z)} A_{4(r)}}$$

$$\times \frac{\partial}{\partial z} \left\{ \int_0^r \left[\int_r^{R_*} \frac{1}{r^3} \left(\int_0^r 2\pi A_{1(z)} A_{2(r)} r \, \mathrm{d}r \right)^2 \mathrm{d}r \right] r \, \mathrm{d}r \right\} \mathrm{d}r \tag{32}$$

In our experiments, u_∞ is much smaller than u_0 and can be neglected. Thus,

$$u_0 \cong \frac{\mu_e I^2}{4\pi^2 T_0 M} K \left(A_{1(z)}, A_{3(z)}, R^*_{(z)} \right) \tag{33}$$

From Eq. (33), velocity head can be solved:

$$\frac{1}{2} \rho_0 u_0^2 = \frac{1}{2} \rho_0 \frac{\mu_e^2 I^4}{(4\pi^2)^2 T_0^2 M^2} K^2 \tag{34}$$

If the plasma mainly consists of electrons and primary ions, we have

$$\rho = m_i n_i \cong m_i (n/2) \tag{35}$$

Using $n = P/kT$, we have

$$\rho \cong \tfrac{1}{2} (P m_i / kT) \tag{36}$$

At the axes of the arc, we have

$$\rho_0 \cong \tfrac{1}{2} (P/k)(m_i / T_0) \tag{37}$$

Substitution of Eq. (37) into Eq. (34) results in

$$\frac{1}{2} \rho_0 u_0^2 \cong \frac{1}{4} \frac{P \mu_e^2 m_i K^2}{(4\pi^2)^2 k M^2} \frac{I^4}{T_0^3} \tag{38}$$

If it is supposed that the radial distribution of the temperature satisfies the parabola distribution, the temperature T_0 at the axes of the arc can be determined by Eq. (4). Thus,

$$\tfrac{1}{2} \rho_0 u_0^2 \cong \theta I^2 \tag{39}$$

into that,

$$\theta = \tfrac{1}{4} \left(P \mu_e^2 m_i K^2 R^{*4} E^2 \right) / \left[(4\pi^2)^2 \times (1.041 \times 10^3)^3 k M^2 \right] \tag{40}$$

The excess total pressure is

$$P_{\Sigma\mathrm{theo}(z)} = P_{0(z)} + \tfrac{1}{2} \rho_0 u_{0(z)}^2 - P_{\infty(z)} \tag{41}$$

Thus, adding the velocity head to the excess static pressure head, we obtain the axial excess total pressure head

$$P_{\Sigma\mathrm{theo}(z)} = \left(\mu_e I^2 / 2\pi \right) \aleph_{(R^*)} + \theta I^2 \tag{42}$$

where $\aleph_{(R^*)}$ is defined in Eq. (20).

When the parameters in Eq. (40) are analyzed, it is apparent that θ is the function of z and R^*, R^* has fixed relation with z, and the relation keeps consistency at different open-circuit voltages, according to our experiments. Thus, θ is the function of R^*. Equation (42) can be expressed as follows:

$$P_{\Sigma\text{theo}(z)} = \left[(\mu_e/2\pi)\aleph_{(R*)} + \theta_{(R^*)}\right] I^2 \tag{43}$$

In fact, the current I is pulsant according to the experiments, and so is the corresponding P_Σ. It is reputed that P_Σ, measured by the pressure transducer, is a time-averaged value. Thus according to the experiments, the current can be approximately represented as the sum of the time-averaged value and the sine pulse component:

$$I = \bar{I} + \tilde{I} \sin \omega t \tag{44}$$

Substituting Eq. (44) into Eq. (43), we obtain

$$P_{\Sigma\text{theo}(z)} = \left[(\mu_e/2\pi)\aleph_{(R^*)} + \theta\right](\bar{I} + \tilde{I} \sin \omega t)^2 \tag{45}$$

Integrating Eq. (45) for a cycle results in

$$\int_0^{2\pi} P_{\Sigma\text{theo}(z)}\, \mathrm{d}\omega t = \int_0^{2\pi} \left[\frac{\mu_e}{2\pi}\aleph_{(R^*)} + \theta\right](\bar{I} + \tilde{I} \sin \omega t)^2\, \mathrm{d}\omega t \tag{46}$$

The experiments indicate that R^* does not change with the pulsation amplitude of the current. Thus, the value in the bracket can be regarded as a constant. Then the time-averaged excess total pressure is obtained:

$$\frac{1}{2\pi}\int_0^{2\pi} P_{\Sigma\text{theo}(z)}\, \mathrm{d}\omega t = \left[\frac{\mu_e}{2\pi}\aleph_{(R^*)} + \theta\right]\left(\bar{I}^2 + \frac{1}{4\pi}\tilde{I}^2\right) \tag{47}$$

Equation (47) is the result of the theoretical analysis. The item $(\mu_e/2\pi)\aleph_{(R^*)} + \theta$ in Eq. (47) is pertinent to the magnetic permeability of the plasma, the distribution of the current density, and the distribution of the arc temperature, which are difficult to measure. Therefore, it is difficult to give quantitative results, but the qualitative result is given according to Eq. (47) and can explain the result in Fig. 4 qualitatively. In Fig. 4, when the open-circuit voltage is same, for example, the open-circuit voltage is 148 V, the average excess total pressure increases with rising of the average current. When the average current is same, the larger open-circuit voltage leads to the larger average current alternating component and the larger excess total pressure.

V. Conclusions

The alternating component significantly influences the arc characteristic. It influences the inner flow of the arc, the arc blow force on the anode, and the heat transfer to the anode. Larger alternating component leads to larger arc blow force. Thus, the efficiency of the heat transfer to the anode increases.

References

[1]Pfender, E., "Thermal Plasma Technology: Where Do We Stand and Where Are We Going?," *Plasma Chemistry and Plasma Processing,* Vol. 19, No. 1, 1999, pp. 1–31.

[2]Vinayo, M. E., Kassabji, F., Guyonnet, J., and Fauchais, P., "Plasma Sprayed WC-Co Coatings: Influence of Spray Conditions (Atmospheric and Low Pressure Plasma Spraying) on the Crystal Structure, Porosity, and Hardness," *Journal of Vacuum Science and Technology*, Vol. 3, No. 6, 1985, pp. 2483–2489.

[3]Rukov, M. F., Koroteev, A. S., and Wrukov, B. A., "Physical and Aerodynamic Process in Plasma Torch," *Applied Dynamics of Thermal Plasma*, 1st ed., Science Press, Siberia, 1975, pp. 19–67 (Chinese translation).

[4]Planche, M. P., Duan, Z., Lagnoux, O., Heberlein, J., Fauchais, P., and Pfender, E., "Study of Arc Fluctuations with Different Plasma Spray Torch Configurations," *Proceedings of the 13th International Symposium on Plasma Chemistry*, Vol. 3, 1997, pp. 1460–1465.

[5]Singh, N., Razafinimanana, M., and Hlina, J., "Characterization of a DC Plasma Torch through Its Light and Voltage Fluctuations," *Journal of Physics D: Applied Physics*, Vol. 33, No. 3, 2000, pp. 270–274.

[6]Desven, S. V., "The Thermal and Aerodynamic Diagnostic Methods of Plasma," *Physics and Technology of Low-temperature Plasma*, 1st ed., Atomic Energy Press, Moscow, 1972, pp. 147–150 (Chinese translation).

[7]Pfender, E., Fincke, J., and Spores, R., "Entrainment of Cold Gas into Thermal Plasma Jets," *Plasma Chemistry and Plasma Processing,* Vol. 11, No. 4, 1991, pp. 529–543.

[8]Zhao, W., Tian, K., Liu, D., and Zhang, G., "Fluctuation Phenomenon Analysis of Arc Plasma Spraying Jet," *Chinese Physics Letters*, Vol. 18, No. 8, 2001, pp. 1092–1094.

[9]Rukov, M. F., Koroteev, A. S., and Wrukov, B. A., "Stability of the Arc," *Applied Dynamics of Thermal Plasma*, 1st ed., Science Press, Siberia, 1975, pp. 300–305 (Chinese translation).

[10]Gross, B., Grycz, B., and Miklossy, K., "Conditions of a Stable Arc," *Plasma Technology*, 1st ed., Iliffe Books, London, 1968, pp. 167–171.

[11]Gross, B., Grycz, B., and Miklossy, K., "Calculating the Plasma Temperature of a Water-Stabilized Electric Arc," *Plasma Technology*, 1st ed., Iliffe Books, London, 1968, pp. 241–243.

[12]Cohen, S., Spitzer, L., and Routly, M. P., "The Electrical Conductivity of an Ionized Gas," *Physical Review*, Vol. 80, No. 2, 1950, pp. 230–238.

[13]Burnhorn, F., and Maecker, H., "Feldstarkemessungen an Wasserstabilisierten Hochleistungsbogen," *Zeitschrift Für Physik*, Vol. 129, 1951, pp. 369–376.

[14]Boyd, T. J. M., and Sanderson, J. J., "Relaxation Times," *Plasma Dynamics*, 1st ed., Vol. 1, Thomas Nelson, London, 1969, pp. 289–293.

[15]Admur, J., and Mason, E., "Properties of Gases at Very High Temperatures," *Physics of Fluids*, Vol. 1, No. 2, 1958, pp. 370–383.